Mixed gas diffusion and permeation of ternary and quaternary CO2/CO/N2/O2 gas mixtures in Matrimid®, polyetherimide and poly(lactic acid) membranes for CO2/CO separation

Mixed gas diffusion and permeation of ternary and quaternary $CO_2/CO/N_2/O_2$ gas mixtures in Matrimid®, polyetherimide and poly(lactic acid) membranes for CO_2/CO separation

R. Checchetto[(1,*)], M. Scarpa[(1)], M.G. De Angelis [(2)], M. Minelli[(3)]

[(1)] Dipartimento di Fisica - Università di Trento, Via Sommarive 14, I-28132 Povo (TN), Italy

[(2)] School of Engineering, University of Edinburgh, Sanderson Building, EH93FB, Edinburgh, UK

[(3)] Department of Civil, Chemical, Environmental and Materials Engineering, Alma Mater Studiorum – University of Bologna, via Terracini 28, I-40131 Bologna, Italy

(*) e-mail: riccardo.checchetto@unitn.it ; grazia.deangelis@ed.ac.uk

Abstract

The CO_2/CO mixed-gas separation performance of a polyimide (Matrimid®), polyetherimide (PEI) and polylactic acid (PLA) membrane, were characterized in the presence of CO_2- rich ternary ($CO_2/CO/O_2$) and quaternary ($CO_2/CO/O_2/N_2$) feed gas mixtures mimicking the products of CO_2 reforming conversion reactions. The membrane- based separation of this mixture is poorly characterized and original data were obtained in a novel mass spectrometric apparatus that permits to monitor the instantaneous permeate composition, thus allowing to evaluate both mixed gas diffusion and permeability coefficients of all gases. CO_2, CO, O_2 and N_2 permeability and diffusivity in single gas tests were measured between 298 and 353 K up to 1 atm feed pressure and relevant activation energies were evaluated. At 298 K Matrimid® exhibits CO permeability of 0.50 ± 0.03 Barrer and an ideal CO_2/CO selectivity of 16 ± 1. PEI and PLA exhibit similar ideal selectivity values but lower CO transport rates. In all examined polymer films the CO_2/CO selectivity has absorption-selective character that favours the permeation of CO_2. The ideal CO_2/CO selectivity of all membrane samples decreases with temperature, reaching values of 10 ± 1 at 335 K in Matrimid®. The CO_2/CO selective performances of all examined membrane do not show markable variations exposing the membrane samples to CO_2- rich gas mixtures as feed gas. The upper bound correlation among selectivity and permeability for the CO_2/CO gas couple is here for the first time proposed.

Keywords:

Polymeric membranes; CO_2 plasma reforming; Mixed gas permeation/diffusion at different temperatures; CO transport; CO_2/CO separation mechanism.

1. Introduction

CO_2 reforming by non-thermal plasma (NTP) conversion is an emerging technique for CO_2 recycling. A non-thermal plasma operates at room temperature and atmospheric pressure generating highly active molecular/atomic species and energetic electrons with 1 to 10 eV energy: when electrons with energy in this interval value collide with molecules, excite them and break chemical bonds. CO_2 dissociation occurs by $CO_2 \rightarrow CO + \frac{1}{2}O_2$ reaction and requires only 5.5 eV; dissociation proceeds via stepwise vibrational excitation that breaks the $OC = O$ bond [1,2]. When driven by renewable energy, this innovative CO_2 conversion process would be an important step towards a sustainable energy scenario: it allows, in fact, CO_2 recycling with the simultaneous storage of the electricity produced by the renewable sources in form of chemical fuels offering a solar-to-fuel efficiency close to 23 % [1,2]. Its implementation requires anyway the upgrading of the resulting gas mixture by separation of the unconverted CO_2 molecules from CO [1,2].

Compared to the commercial separation technologies of Swing Adsorption or Cryogenic Distillation, membrane processes are of particular interest offering low energy consumption, high sustainability and environmentally friendly character [3,4]. Gas transport through a polymeric membrane occurs when a pressure difference is applied between the membrane opposite sides: the gas mixture components are separated because different gas species permeate through the membrane layers at different rates depending on their solubility and diffusivity in the polymeric layers [4]. There is very little knowledge on the CO transport properties and CO_2/CO separation performances of commercial polymeric gas separation membranes. Such information would be of importance not only for CO separation from mixtures produced by CO_2 reforming, but also for separation of mixtures produced in processes such as partial oxidation of carbon- containing materials (coal and biomasses) or by steam reforming of natural gas [5].

In this work we present a detailed study on the CO transport properties and CO_2/CO separation performances in multicomponent state of polymeric membranes exposed to CO_2- rich gas mixtures having composition similar to those produced by CO_2 reforming by NTP conversion. The tests were carried out with a novel experimental mass spectrometric apparatus which allows to monitor the transient and steady-state multicomponent transport of gas mixtures in polymeric membranes with high accuracy, allowing to determine the mixed gas diffusion and permeation coefficients, which are extremely rare and time-consuming, as recent studies reveal [6]. Tests were carried out using dense Matrimid®, polyetherimide (PEI) and polylactic acid (PLA) membrane films. Matrimid® is an aromatic polyimide with glassy structure exhibiting high thermal stability ($T_g =$

$302°C$) and acceptable values of selectivity and permeability for CO_2/CH_4 separation and H_2 purification applications [7]. PEI is an amorphous thermoplastic with glass transition temperature at 217°C, decomposition temperature at 427°C and 1.27 g/cm^3 density offering excellent chemical resistance and high strength [8]. PLA is a "green" innovative aliphatic polyester having 1.24 g/cm^3 density and 160°C melting point that is produced from the fermentation of renewable resources such as crops studied for packaging applications as substitute of commercial petroleum- derived polymers [9]. Matrimid® and PEI were chosen for this study because these commercial polymers are used for the construction of hollow fiber membranes employed in industrial plants for biogas upgrading [10,11] and it is thus of interest a study on their CO_2/CO separation properties. PLA was chosen because the transport properties of various gases in this biopolymer are of interest for its envisaged applications [9] and no information is currently present regarding the CO permeation process.

The aim of this paper is to present original data on the CO permeability and diffusivity in the examined polymer samples and analyze their CO_2/CO selective properties at different temperatures. Separate information on gas permeability and diffusivity in the examined samples will be presented to underline the mechanism responsible of the membrane separation properties. Permeation tests were carried out in single gas and in mixed gas conditions: the comparison between single gas transport and gas mixture transport is of great importance because when the membrane is exposed to gas mixtures, as it occurs in real operative conditions, microscopic phenomena such as competitive sorption effects, plasticization processes and matrix dilation affect the transport of gas mixture components and the membrane selectivity values can thus differ from the ideal ones [12].

2. **Experimental**

2.1 **Materials**

Matrimid® films with thickness of 60 $\pm$ 2 μm were prepared dissolving polyimide powders (kindly provided by Huntsman Advanced Materials) in dichloromethane (Sigma-Aldrich) (1.5 wt. %) and the resulting solution was casted in a petri dish; after solvent evaporation in a clean hood overnight, the resulting film was inserted in a vacuum oven at 200°C overnight.

Polyetherimide (PEI) films with thickness of 80 $\pm$ 2 μm were prepared dissolving 0.65 g polyetherimide pellets with density 1.27 g/cm^3 (Sigma-Aldrich, Milan) in 40 mL $CHCl_3$. The solution was heated to about 40-50°C and kept under stirring until complete dissolution. Then it was casted

on glass dishes, dried at RT for 5 days, then in an oven at 60°C for 24 h and finally in a desiccator under mild vacuum until utilization.

Nearly amorphous PLA films with thickness of 50 ± 2 μm were prepared dissolving PLA pellets (Nature Works LLC, PLA 4032D) in chloroform (1 g PLA / 25 ml $CHCl_3$) at 40°C under magnetic stirring until completely dissolved. Film samples were obtained casting the resulting solution in a petri dish; the solvent was let evaporate first at room temperature for 24 hours and then for 4 hours in a ventilated oven at 40° C. DSC analysis not reported here revealed that the crystalline content of the present film samples was lower than 3 %.

We studied the transport of carbon dioxide (CO_2), carbon monoxide (CO), nitrogen (N_2), synthetic air (a dry mixture of 20 vol. % O_2 and 80 vol. % N_2) and of two gas mixtures, M224 and M225, whose composition is reported in Table I. These mixtures were prepared by a static method introducing known amounts of single gas components into a previously evacuated rigid vessel; their composition mimics that of mixtures resulting from CO_2 plasma reforming [13,14].

	CO_2 (vol %)	CO (vol %)	O_2 (vol %)	N_2 (vol %)
M224	64 ± 1	26 ± 1	9 ± 1	-
M225	30 ± 1	26 ± 1	9 ± 1	34 ± 1

TABLE I: Composition of the ternary (M224) and quaternary (M225) gas mixtures.

The molecular diameters (σ_k) and critical temperatures (T_c) of test gases are reported in Table II [15]. Gas transport tests were carried out at temperature and feed pressure values relevant for CO_2 plasma reforming processes, namely $T < 100$°C and $p_{feed} < 10^5$ Pa.

gas	σ_k (pm)	σ_{LJ} (pm)	σ_C (pm)	V_c (cm^3/mol)	T_c (K)	γ_α (A/Pa)	s_p (m^3/s)
CO_2	330	394	365	91.9	304.19	6.71×10^{-3}	130 ± 2
CO	376	369	363	90.1	132.91	5.91×10^{-3}	140 ± 2
N_2	364	380	361	89.4	126.2	5.63×10^{-3}	125 ± 2
O_2	346	345	339	73.5	154.6	4.54×10^{-3}	135 ± 2

TABLE II: Kinetic diameters (σ_k), Lennard-Jones diameters (σ_{LJ}), Chung diameter (σ_C), critical molar volume (V_c) and temperatures (T_c) of the examined test gases [15]. The last two columns report the QMS sensitivity γ_α and the pumping speed of our vacuum system for each gas specie. Values of the β parameters are: $\beta(CO^+/CO_2)$ = 0.099 and $\beta(N^+/N_2)$ = 0.103. Experimental indetermination of the γ_α and β parameters is ~ 1 % [16].

2.2 **Gas transport tests**

The description of the experimental apparatus and of the procedure for the analysis of the gas mixture transport kinetics through polymeric membranes is reported in a previous paper [16]. Permeation tests were carried out by gas-phase permeation technique in dead-end configuration. At time $t = 0$ the feed side of the membrane sample is exposed to the feed gas at total pressure $p_{feed} = \sum_\alpha p^\alpha_{feed}$; in the previous relation p^α_{feed} is the partial pressure value of the gas specie α. Penetrant molecules permeate through the membrane in a vacuum chamber of volume V and temperature T_{ch}; these molecules form in this volume a gas mixture having total pressure $p(t) = \sum_\alpha p_\alpha(t)$. The partial pressure of the permeated α molecules, $p_\alpha(t)$, changes with time t according to the relation:

$$\frac{1}{R\,T_{ch}}\left[V\frac{dp_\alpha(t)}{dt} + s_p\,p_\alpha(t)\right] = A\,j_\alpha(t) \quad (1)$$

where R is the universal gas constant, s_p the effective pumping speed of the vacuum system. In the previous relation $j_\alpha(t)$ is the permeation flux of the α gas specie and A the membrane surface area. Tests were carried out with the analysis chamber under dynamic pumping conditions using a vacuum system based on turbo-molecular pumps [16]. When the condition $\frac{s_p}{V} \gg \frac{1}{p_\alpha(t)}\frac{dp_\alpha(t)}{dt}$ is satisfied then $p_\alpha(t)$ is a measure of the permeation flux $j_\alpha(t)$ of the α gas specie by the relation:

$$j_\alpha(t) = \frac{1}{A}\,\frac{1}{R\,T_{ch}}\,s_p\,p_\alpha(t) \quad (2)$$

In our experimental approach we measured $p_\alpha(t)$ as a function of time t with a calibrated Quadrupole Mass Spectrometer (QMS) equipped with a grid- type ion source and a 90° off-axis Secondary Electron Multiplier (SEM) for ion detection.

This instrument was calibrated by the following procedure [16]. We injected pure gas α in the continuously pumped permeation chamber through a variable leak valve and recorded the $i(\alpha^+/\alpha)$ and $i(\alpha_i^+/\alpha)$ QMS ion currents pertinent to the singly charged molecular ion (α^+/α) and its fragmentation ions (α_i^+/α). After background subtraction, the QMS sensitivity γ_α for the test gas α was obtained as:

$$\gamma_\alpha = \frac{i(\alpha^+/\alpha)}{p_\alpha} \quad (3)$$

while the QMS sensitivity for the (α_i^+/α) fragmentation ion relative to that of the (α^+/α) ion by the relation:

$$\beta(\alpha_i^+/\alpha) = \frac{i(\alpha_i^+/\alpha)}{i(\alpha^+/\alpha)} \quad (4)$$

Values of the γ_α, $\beta(\alpha_i^+/\alpha)$ and of the s_p parameters are reported in Table II. Calibration procedures and pertinent validation tests are presented in ref. [16].

In single gas tests we exposed the membrane samples to the α gas specie and recorded the $i(\alpha^+/\alpha)$ ion current which represents the net mass signal $s_\alpha(t)$; the partial pressure $p_\alpha(t)$ in the permeation chamber of this gas specie was then evaluated by eq. 3 and the permeation flux transient $j_\alpha(t)$ by eq. 2. As an example in fig. SI1 we report the $s_\alpha(t)$ signals obtained with the PLA membrane films while in fig. 1 we report the corresponding $j_\alpha(t)$ curves obtained converting sampled $s_\alpha(t)$ data by eq. 2 using parameters in Table II.

In mixed gas tests we recorded, for each α gas specie forming the feed mixture, the pertinent $i(\alpha^+/\alpha)$ and $i(\alpha_i^+/\alpha)$ ion currents. The net mass signal, $s_\alpha(t)$, was then obtained as follows. The $s_{CO_2}(t)$ and $s_{O_2}(t)$ signals are unambiguously given by the $i(CO_2^+/CO_2)$ and $i(O_2^+/O_2)$ QMS ion currents having mass-charge ratio $m/e = 44$ and $32\ Da$, respectively. The $s_{N_2}(t)$ signal was obtained monitoring the $s_N(t) = i(N^+/N_2)$ ion current ($m/e = 14$ Da) resulting from the N^+ ions formed in the electron- impact fragmentation of the N_2 molecules: $s_{N_2}(t) = s_N(t)/\beta(N^+/N_2)$. In our experimental mixed gas tests, the $i(m/e = 28\ Da)$ ion current is given by three contributions: the contribution of the (CO^+/CO) ions formed in the ionization of the carbon monoxide molecule, the contribution of the (CO^+/CO_2) ions formed upon electron- impact fragmentation of CO_2 molecules and the contribution from the (N_2^+/N_2) ions. The net CO mass signal, $s_{CO}(t)$, was obtained subtracting the signal $\varphi_{CO} = \beta(CO^+/CO_2)\, i(CO_2^+/CO_2) + s_N(t)/\beta(N^+/N_2)$ from the $i(m/e = 28\ Da)$ ion current: $s_{CO}(t) = i(m/e = 28\ Da) - \varphi_{CO}$ [16]. As examples to illustrate the procedure, in the Supplementary Information Section, we report in figs. SI2 and SI3 the $s_\alpha(t)$ signals obtained in permeation tests exposing the PEI membrane to the M224 gas mixture at $T = 300 \pm 2$ K (fig. SI2) and the Matrimid® membrane film to the M225 gas mixture at $T = 300 \pm 2$ K (fig. SI3). The partial pressure $p_\alpha(t)$ in the permeation chamber of each gas specie forming the gas mixture was then evaluated by eq. 3 and its permeation flux transient $j_\alpha(t)$ by eq. 2. Figs. 2 and 3 report as symbols the $j_\alpha(t)$ permeation curves obtained using sampled $s_\alpha(t)$ data of fig. SI2 and SI3.

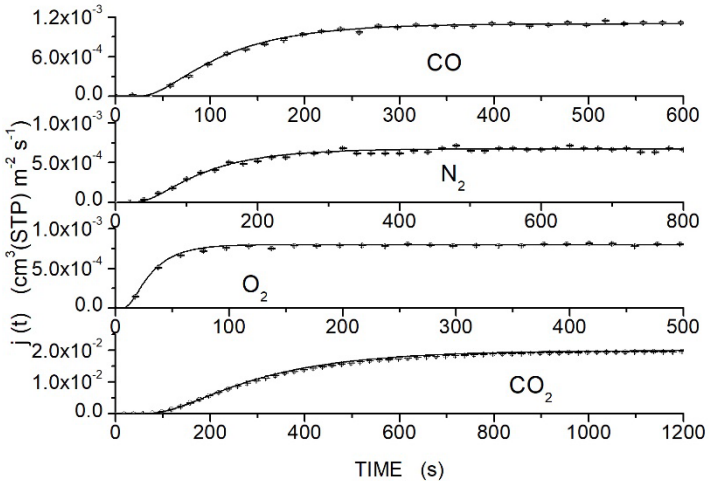

Fig. 1: $j_\alpha(t)$ permeation curves obtained with the PLA membrane samples exposed to pure gases CO_2, CO and N_2 gas ($p_{feed} = 45 \pm 1$ kPa) and to the dry N_2/O_2 gas mixture ($p_{feed} = 72 \pm 1$ kPa) at $T = 300 \pm 2$ K. Curves were calculated converting sampled $s_\alpha(t)$ data of fig. SI1 by eq. 2.

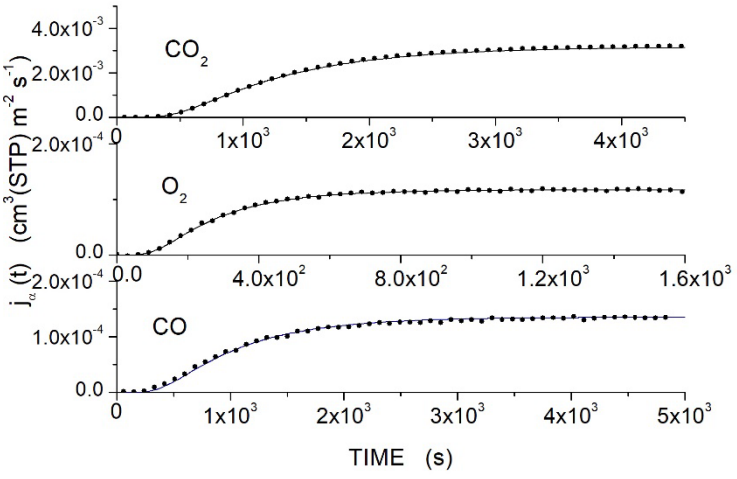

Fig. 2: $j_\alpha(t)$ permeation curves obtained with the PEI membrane samples exposed to the M224 gas mixture ($p_{feed} = 45 \pm 1$ kPa) at $T = 300 \pm 2$ K. Curves were calculated converting sampled $s_\alpha(t)$ data of fig. SI2 by eq. 2.

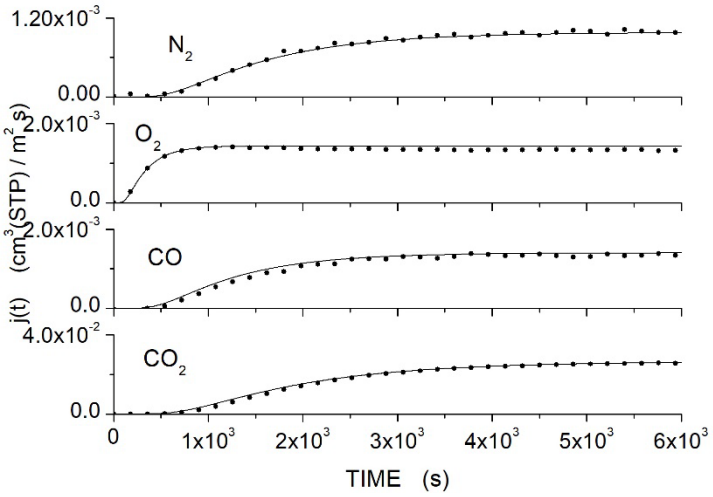

Fig. 3: $j_\alpha(t)$ permeation curves obtained with the Matrimid® membrane samples exposed to the M225 gas mixture ($p_{feed} = 72 \pm 1$ kPa) at $T = 300 \pm 2$ K. Curves were calculated converting sampled $s_\alpha(t)$ data of fig. SI3 by eq. 2.

3. Results and discussion

3.1 Data analysis

The experimental $j_\alpha(t)$ permeation curves, as obtained in single and mixed gas conditions, were analysed assuming that the permeation process obeys to the solution-diffusion mechanism [17]. According to this mechanism, when the feed side of a homogeneous membrane of thickness L is exposed at time $t = 0$ to the feed gas kept at pressure p^α_{feed}, gas molecules are absorbed in the membrane surface layers and their concentration here, c_α, immediately reaches the equilibrium value ~~given by the Henry law~~: $c_\alpha = S_\alpha\, p^\alpha_{feed}$ where S_α is the gas solubility in the polymeric membrane layers. Absorbed molecule diffuse through the membrane layers to the opposite side down to their concentration gradient according to the Fick's law and are here desorbed [17]. The kinetics of the permeation process is described by the following relationship [18], valid for a constant diffusion coefficient:

$$f_\alpha(t) = F_\alpha \left[1 + 2\sum_{n\geq 1}(-1)^n\, e^{-\frac{D_\alpha n^2 \pi^2 t}{L^2}}\right] \qquad (5)$$

$$F_\alpha = \frac{D_\alpha}{L} S_\alpha p^\alpha_{feed} = \frac{P_\alpha}{L} p^\alpha_{feed} \qquad (6)$$

in which $f_\alpha(t)$ is the permeation flux as a function of time t (flux transient), D_α is the gas diffusivity in the membrane layers and F_α the permeation flux of the α gas specie in stationary transport conditions. The parameter $P_\alpha = D_\alpha\, S_\alpha$ is the membrane gas permeability.

This approach permits to evaluate separately the penetrant permeability and diffusivity. The values of the P_α and D_α transport parameters were, in fact, obtained as follows: P_α was calculated measuring the permeation flux of the α gas specie in stationary transport conditions, J_α, and using eq. 6 while the D_α value by best fitting the experimental $j_\alpha(t)$ curves by eq. 5. In single-gas conditions the p^α_{feed} value in eq. 5 is the total pressure of the feed gas while in mixed gas conditions (and with synthetic air) p^α_{feed} is the partial pressure of the α gas specie in the feed mixture ($p_{feed} = \sum_\alpha p^\alpha_{feed}$).

3.2 Permeation tests

In the upper panel of fig. 4 we present, as an example, the $j_{CO}(t)$ permeation curves obtained at $T = 295$ K in single gas tests exposing the Matrimid® membrane sample to carbon monoxide (CO) at different feed pressure values. In the lower panel of this figure the value of $j_{CO}(t)$ flux in stationary transport conditions (J_{CO}) is reported as a function of the CO feed pressure, p^{CO}_{feed}. The linear relationship between J_{CO} and p^{CO}_{feed} evidences that in this pressure interval the CO transport through the Matrimid® membrane film has a constant permeability coefficient, as reasonable due to the low-pressure range inspected: similar trend was observed also with the PEI and PLA membranes. From similar sets of permeation curves, the P_α and D_α values were evaluated as average value of the permeability and diffusivity values obtained in each test while their uncertainty as values semi-dispersion.

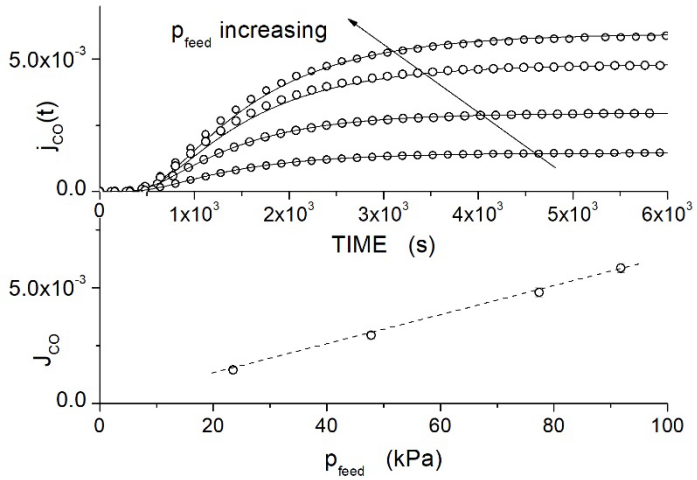

Fig. 4: Upper panel: $j_{CO}(t)$ curves obtained at $T = 295$ K in single gas tests exposing the Matrimid® membrane sample to carbon monoxide at different feed pressure values [units: cm^3(STP) / m^2 s]. Lower panel: value of the $j_{CO}(t)$ flux in stationary transport conditions (J_{CO}) as a function of the CO feed pressure [units of j_{CO}: cm^3(STP) / m^2 s].

The Arrhenius plot of the P_α and D_α values obtained in single gas permeation tests is reported in the left panel of fig. 5 for Matrimid®, of fig. 6 for PEI and of fig. 7 for PLA; the right panels report data obtained exposing the membrane samples to the M224 gas mixture. The gas solubility values S_α calculated by the relation $S_\alpha = P_\alpha / D_\alpha$ using P_α and D_α data pertinent to single gas test for the CO_2 and CO penetrant molecules are reported in Fig. 8.

The numerical values of the gas transport parameters in figs. 5-8 can be found in the Supplementary Information Sections together with data obtained with the M225 gas mixture, see Tabs. SI1-SI3. N_2 diffusivity values in Matrimid® and PEI are equal, within the experimental indetermination, to CO diffusivity values (see Tabs. SI1 and SI2) and are thus not reported in the right panels of figs. 5 and 6.

At each examined temperature, the following trend holds for the permeability coefficients: $P_{CO_2} > P_{O_2} > P_{CO} \sim P_{N_2}$ and the following for the diffusion coefficients: $D_{O_2} > D_{CO} \sim D_{N_2} > D_{CO_2}$.

The observed diffusivities are within the same order of magnitude, as the size of the four penetrant molecules are comparable (see Table II). Therefore the correlation between diffusion coefficient and molecular dimension may be cumbersome and depends on what type of metrics is considered. Interestingly, D values seem to correlate better considering the critical molecular volume rather than the kinetic diameter.

We also observe that increasing temperature the permeability and diffusivity values increase: such increase is nearly negligible for the glassy PEI film and results more marked for the diffusivity than for the permeability values.

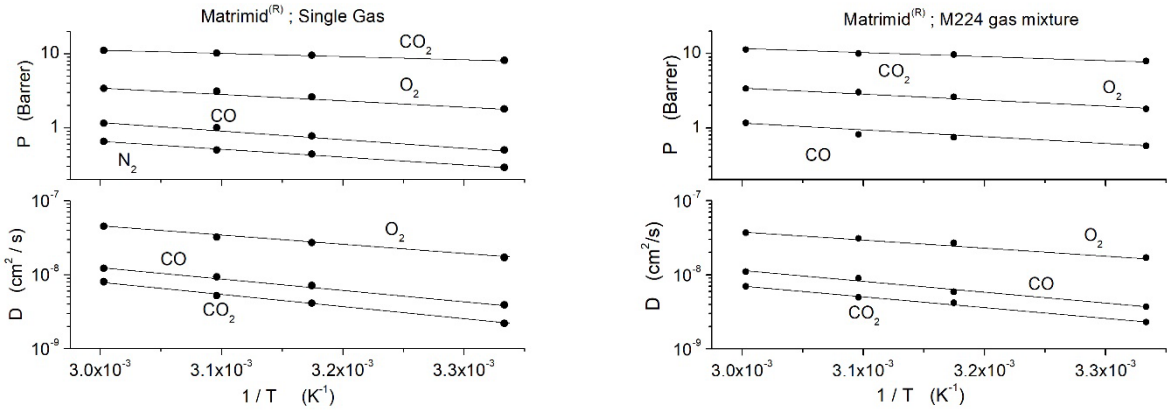

Fig. 5: Arrhenius plot of the gas permeability (P) and diffusivity (D) of the Matrimid® membrane sample as obtained in single gas permeation tests (left panel) and with the ternary M224 gas mixture (right panel). Numerical values are reported in the Supplementary Information section. N_2 diffusivity values measured in Single Gas conditions (left panel) are not reported as overlap with CO diffusivity values.

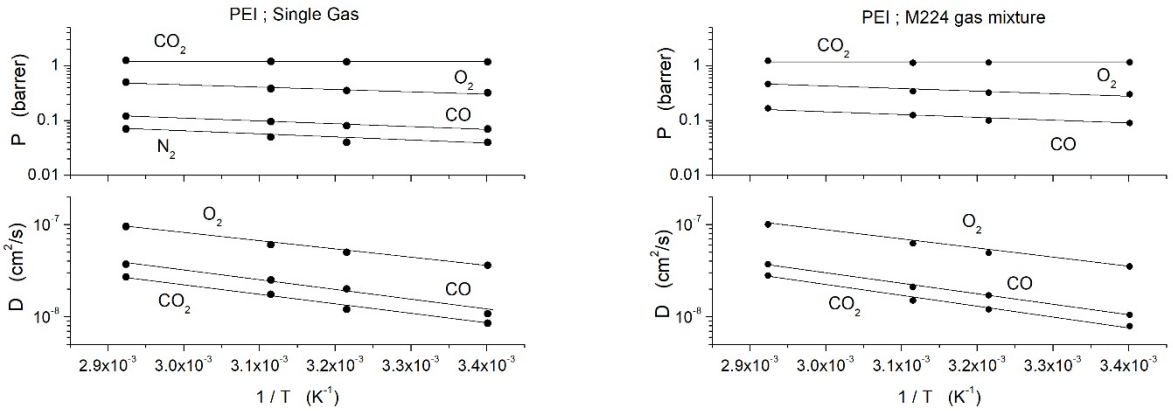

Fig. 6: Arrhenius plot of the gas permeability (P) and diffusivity (D) of the PEI membrane sample as obtained in single gas permeation (left panel) and with the ternary M224 gas mixture (right panel). Numerical values are reported in the Supplementary Information section. N_2 diffusivity values measured in Single Gas conditions (left panel) are not reported as overlap with CO diffusivity values.

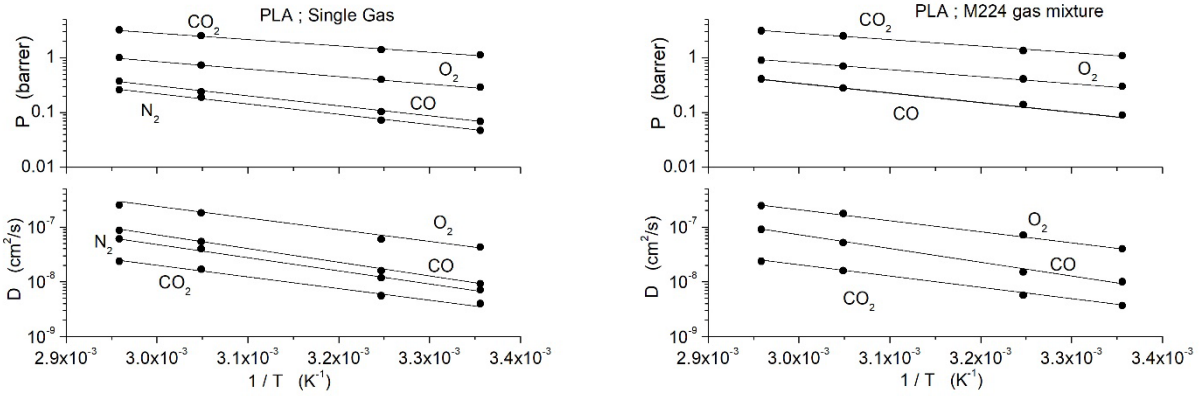

Fig. 7: Arrhenius plot of the gas permeability (P) and diffusivity (D) of the PLA membrane film as obtained in single gas permeation tests (left panel) and with the ternary M224 gas mixture (right panel). Numerical values are reported in the Supplementary Information section.

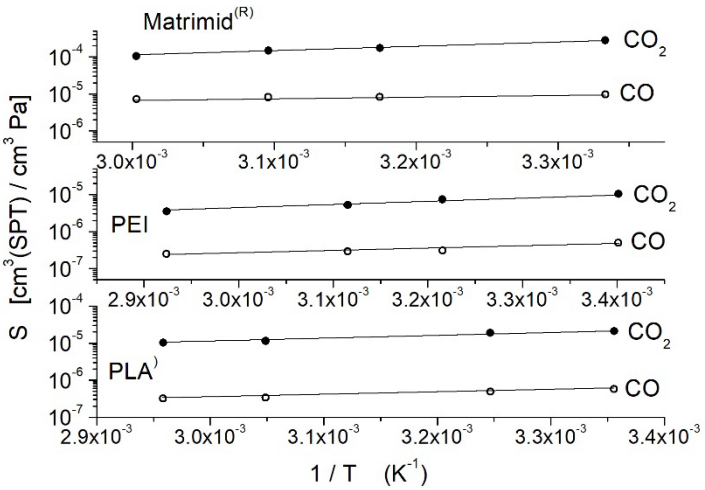

Fig. 8: Arrhenius plot of the gas solubility (S) of the Matrimid®, PEI and PLA membrane film in single gas permeation tests obtained using P and D data in the left panels of figs. 4-6 by the relation $S = P/D$. Numerical values are reported in the Supplementary Information section.

The activation energy values obtained by fitting permeability and diffusivity data in the left panels of figs. 5-7 by the Arrhenius equation are reported in Table III and IV, respectively.

E_P (kJ/mol)	CO_2	N_2	O_2	CO
Matrimid®	7.7 ± 0.5	20.3 ± 0.8	16 ± 1	20.7 ± 0.9
PEI	1.0 ± 0.2	10 ± 1	8 ± 1	9.3 ± 0.5
PLA	22.4 ± 0.5	36.9 ± 0.7	25.1 ± 0.8	36 ± 1

TABLE III: Activation energy values for permeation obtained in single gas tests fitting P_α data in in the left panels of Figs. 5-7.

E_D (kJ/mol)	CO_2	N_2	O_2	CO
Matrimid®	32.5 ± 0.4	29.5 ± 0.3	24.5 ± 0.8	28.7 ± 0.9
PEI	20.0 ± 0.6	21.9 ± 0.7	16.7 ± 0.5	21.9 ± 0.7
PLA	39 ± 1	46 ± 1	39 ± 1	47 ± 1

TABLE IV: Activation energy values for diffusion obtained in single gas tests fitting D_α data in the left panels of Figs. 5-7.

Because only few studies exist on the permeability of the CO penetrant in polymeric membranes and no one reports separate values of CO permeability and diffusivity in the examined polymeric membranes, it is worthy to compare transport data obtained with the CO_2, N_2 and O_2 penetrants with literature values to assure the reliability of our experimental approach. Tabs. V, VI and VII present values of gas transport parameters obtained in single gas conditions in experimental tests carried out at near-ambient temperature with Matrimid®, PEI and PLA films.

P_{CO2} (barrer)	P_{N2} (barrer)	P_{O2} (barrer)	D_{CO2} (cm^2/s)	D_{N2} (cm^2/s)	D_{O2} (cm^2/s)	Ref.
8.1 ± 0.3	0.29 ± 0.02	1.8 ± 0.1	$(2.2 \pm 0.1) \times 10^{-9}$	$(3.4 \pm 0.2) \times 10^{-9}$	$(1.7 \pm 0.1) \times 10^{-8}$	This work
6.4	0.16	-	-	-	-	19
7.3	0.22	1.46	3×10^{-9}	1×10^{-9}	5×10^{-9}	20
8.9	0.25	1.7	2.9×10^{-9}	2.4×10^{-9}	1.3×10^{-8}	21
9.8	0.31	-	-	-	-	22
7.23	0.21	-	8.9×10^{-9}	4.7×10^{-9}	-	23

TABLE V: Near-ambient temperature of gas permeability and diffusivity of Matrimid® films as measured in single gas permeation tests. Experimental conditions of temperature (T) and trans-membrane pressure (ΔP):

[19] $T = 303$ K, $\Delta P = 2$ to 6 bar; [20] $T = 298$ K, $\Delta P = 2$ bar; [21] $T = 293$ K, $\Delta P = 0.3$ bar; [22] $T = 298$ K, $\Delta P = 4$ bar; [23] $T = 298$ K, $\Delta P = 10$ bar.

P_{CO2} (barrer)	P_{N2} (barrer)	P_{O2} (barrer)	D_{CO2} (cm^2/s)	D_{N2} (cm^2/s)	D_{O2} (cm^2/s)	Ref.
1.17 ± 0.05	0.04 ± 0.01	0.32 ± 0.02	$(8.5 \pm 0.4) \times 10^{-9}$	$(1.00 \pm 0.04) \times 10^{-8}$	$(3.6 \pm 0.1) \times 10^{-8}$	This work
1.27	-	0.6	-	-	-	24
1.32	0.05	0.4	3.7×10^{-9}	-	-	25
1.48	0.05	0.38	-	-	-	26
1.4	0.06	-	-	-	-	27
1.14	-	-	-	-	-	28
1.25	0.05	-	2.5×10^{-9}	2.5×10^{-9}	-	29
0.2 to 0.3	-	-	-	-	-	30
1.46	0.05	0.4	-	-	-	31

TABLE VI: Near-ambient temperature of gas permeability and diffusivity of PEI films as measured in single gas permeation tests. Experimental conditions of temperature (T) and trans-membrane pressure (ΔP): [24] $T = 298$ K, $\Delta P = 0.9$ bar ; [25] $T = 308$ K, $\Delta P = 10$ bar ; [26] $T = 308$ K, $\Delta P = 3.5$ bar ; [27] $T = 308$ K, $\Delta P = 2$ bar ; [28] $T = 308$ K, $\Delta P = 3.5$ bar ; [29] $T = 298$ K, $\Delta P = 2$ to 5 bar ; [30] $T = 298$ K, $\Delta P = 2$ to 6 bar; [31] $T = 308$ K, $\Delta P = 10$ bar.

P_{CO2} (barrer)	P_{N2} (barrer)	P_{O2} (barrer)	D_{CO2} (cm^2/s)	D_{N2} (cm^2/s)	D_{O2} (cm^2/s)	Ref.
1.12 ± 0.05	0.05 ± 0.02	0.29 ± 0.02	$(4.0 \pm 0.2) \times 10^{-9}$	$(7.1 \pm 0.4) \times 10^{-9}$	$(4.3 \pm 0.2) \times 10^{-8}$	This work
1.12	0.04	-	3.76×10^{-9}	7.0×10^{-9}	-	18
1.1	0.05	0.26	4.4×10^{-9}	2.4×10^{-8}	5.7×10^{-8}	32
1.2	0.05	-	4.8×10^{-9}	2.4×10^{-8}	-	33
1.71	-	0.13	-	-	-	34

TABLE VII: Near-ambient temperature of gas permeability and diffusivity of PLA films as measured in single gas permeation tests. Experimental conditions of temperature (T) and trans-membrane pressure (ΔP): [18] $T = 300$ K, $\Delta P = 0.4$ bar; [32] $T = 303$ K, $\Delta P =$ not reported; [33] $T = 308$ K, $\Delta P = 0.5$ to 1 bar; [34] $T = 298$ K, $\Delta P = 1$ bar.

Looking at data in these Tables we can observe good agreement between our experimental data and literature data. Note also that our ideal CO_2/N_2 selectivity value of 28 ± 1 for Matrimid® is coincident with the value of 30 reported in the review of Castro-Munoz *et al.* on Matrimid® [35]. Our ideal CO_2/N_2 selectivity value of 28 ± 1 for PEI well compares with literature PEI values ranging from 25 [27] to 30 [31]. Same consideration holds for our ideal P_{CO2}/P_{N2} selectivity values of 24 ± 1 for PLA which well agrees with the value of 22 reported by Bao *et al.* [32] and with the value of 24 reported by Kamatsuka *et al.* [33].

The comparison of activation energy values in TABLE III and IV with literature data also evidences good compatibility. Activation energy values for permeation in Matrimid® range, in fact, from 5.9 to 9.0 kJ/mol for CO_2 and from 13.6 to 20.2 kJ/mol for N_2 [21,36]; no data was found for the activation energy for diffusion. Good compatibility also exists for PLA data: Bao et al. obtained activation energy value for permeation of 18.5 and 34.6 kJ/mol for CO_2 and N_2, respectively [32] while Auras found a value of 15.7 kJ/mol ~~cor~~ for CO_2 [34]. For E_D in PLA we only found the value of 37 $\pm$ 1 kJ/mol reported by Bao et al. for CO_2 [32]. Concerning PEI, we observe that our activation energy values result lower that those indicated by Vega et al. which reported an activation energy value of 32.8 $\pm$ 1.8 kJ/mol for CO_2 permeation and of 36.0 $\pm$ 0.3 kJ/mol for CO_2 diffusion; the authors reported same values, inside the experimental indetermination, for the respective N_2 activation energies [29].

To discuss the CO_2/CO selective performances of the examined membrane samples, in Tab. V we report the numerical values of the P_α and D_α parameters pertinent to the CO_2 and CO penetrants, as obtained at near-ambient temperature in permeation tests carried out in single and mixed gas conditions. Corresponding values for O_2 and N_2 are reported in the Supplementary Information section, see Tab. SI1-SI3.

		Single Gas	M224	M225
Matrimid®	P_{CO2} (Barrer)	8.1 ± 0.3	7.9 ± 0.3	8.0 ± 0.3
	D_{CO2} (cm²/s)	(2.2 ± 0.1) × 10^{-9}	(2.3 ± 0.1) × 10^{-9}	(2.1 ± 0.1) × 10^{-9}
	P_{CO} (Barrer)	0.50 ± 0.03	0.54 ± 0.03	0.49 ± 0.03
	D_{CO} (cm²/s)	(3.9 ± 0.2) × 10^{-9}	(3.7 ± 0.2) × 10^{-9}	(3.8 ± 0.2) × 10^{-9}
PEI	P_{CO2} (Barrer)	1.17 ± 0.05	1.15 ± 0.05	1.17 ± 0.05
	D_{CO2} (cm²/s)	(8.5 ± 0.4) × 10^{-9}	(8.0 ± 0.4) × 10^{-9}	(8.1 ± 0.4) × 10^{-9}
	P_{CO} (Barrer)	0.07 ± 0.01	0.09 ± 0.01	0.07 ± 0.01
	D_{CO} (cm²/s)	(1.08 ± 0.04) × 10^{-8}	(1.05 ± 0.05) × 10^{-8}	(1.03 ± 0.04) × 10^{-8}
PLA	P_{CO2} (Barrer)	1.12 ± 0.05	1.10 ± 0.05	1.10 ± 0.05
	D_{CO2} (cm²/s)	(4.0 ± 0.2) × 10^{-9}	(3.8 ± 0.2) × 10^{-9}	(3.8 ± 0.2) × 10^{-9}
	P_{CO} (Barrer)	0.07 ± 0.01	0.09 ± 0.01	0.08 ± 0.02
	D_{CO} (cm²/s)	(9.2 ± 0.4) × 10^{-8}	(1.00 ± 0.04) × 10^{-8}	(9.7 ± 0.6) × 10^{-8}

TABLE VIII: Near-ambient temperature values of the CO_2 and CO transport parameters measured in single gas tests and with the M224 and M225 gas mixtures with the examined membrane samples.

The Matrimid® membrane sample exhibits at near-ambient temperature a single gas P_{CO} value of 0.50 $\pm$ 0.03 Barrer which is larger than corresponding value for PEI, 0.07 $\pm$ 0.01 Barrer, and for PLA, 0.07 $\pm$ 0.01 Barrer. The ideal CO_2/CO selectivity values of the examined membrane

films are equivalent inside their experimental uncertainty: at near-ambient temperature, in fact, the ideal CO_2/CO selectivity value is 16 ± 1 for Matrimid®, 17 ± 2 for PEI and 16 ± 2 for PLA. These values are lower than the corresponding ideal CO_2/N_2 selectivity for each membrane sample.

As the temperature increases, the ideal CO_2/CO selectivity of the examined membrane samples decreases (see solid symbols in the upper panels of figs. 9-11) reaching the value of 9.6 ± 0.4 for Matrimid® at 60°C, of 10 ± 1 for PEI at 69°C and of 9 ± 1 for PLA at 65°C. Solid symbols in the lower panel of figs. 10-12 report the D_{CO2}/D_{CO} ratio for the examined membrane samples, as a function of temperature. It can be observed that, in the examined temperature interval, the CO_2 diffusivity is lower than that of CO: the D_{CO2}/D_{CO} ratio is, in fact, ~ 0.6 in Matrimid®, ~ 0.7 in PEI and ~ 0.4 in PLA. We can thus conclude that the CO_2/CO selective properties of all the examined membrane samples have mainly a solution-selective character. Indeed, the larger CO_2 solubility in all examined polymer films is clearly favored by the larger condensability of the CO_2 specie (T_C = 133 K for CO and 304 K for CO_2).

Looking at Tabs. III and IV, we observe that sorption in the examined polymeric films has an exothermic character for both gases. The sorption enthalpy for CO solution $\Delta H_S = E_p - E_D$ is negative and exhibits values of −8 ± 2 kJ/mol for Matrimid®, −13 ± 1 kJ/mol for PEI and −11 ± 2 kJ/mol for PLA: all values lie close to the CO heat of condensation that is − 6 kJ/mol [15]. The ΔH_S values for CO_2 are in absolute value larger, specifically −25 ± 1 kJ/mol for Matrimid®, −19 ± 1 kJ/mol for PEI and −17 ± 1 kJ/mol for PLA, indicating a larger exothermic effect associated with the sorption of such molecule. As a consequence, being the diffusion activation energy similar for the two penetrants, and the D_{CO2}/D_{CO} ratio essentially constant with temperature, the permeability increases with temperature more significantly for CO than for CO_2, resulting in the decrease of the CO_2/CO selectivity with temperature.

Looking at Tab. V we observe that exposing the membrane samples to the ternary, CO_2- rich M224 gas mixture at near-ambient temperature, the P_{CO2} and D_{CO2} values are equal, to within the experimental accuracy, to values obtained in single gas tests. With the PEI and PLA membrane we can observe an apparent slight increase of the P_{CO} value: it's anyway necessary to remark that this increase is of the same order as the experimental uncertainty. The near-ambient temperature CO_2/CO selectivity for the Matrimid® membrane exposed the CO_2- rich ternary M224 gas mixture is similar to the ideal one obtained from pure gas data, 15 ± 1 while it appears slightly decreased with the PEI membrane, 13 ± 2, and with the PLA membrane, 12 ± 2. The P and D parameters

pertinent to ~~N_2 and~~ O_2 obtained with the M224 gas mixture exhibit values equal to those measured in single gas tests. As in single gas tests, by increasing temperature the CO_2/CO selectivity of the examined membrane samples decreases (see open symbols in the upper panel of figs. 9-11) as discussed above and due to the larger exothermic character of CO_2 sorption. In the examined temperature interval, ~~the examined~~ membrane samples exhibit CO_2/CO selectivity values similar to the ideal ones (see figs. 10 and 11).

Open symbols in the lower panel of figs. 9-11 report the D_{CO2}/D_{CO} ratio for the examined membrane samples, as a function of temperature. Comparing permeability and diffusivity data obtained in with the CO_2- rich M224 gas mixture we can conclude that in mixed gas tests the CO_2/CO separation is determined by the different solution properties of the permeants in the matrix, similarly to what happens in single gas processes, in the pressure range inspected. It must be reminded that the pressure considered in the tests was sub-atmospheric to reproduce the conditions encountered in NTP conversion processes.

We also observe that the D_{CO2}/D_{CO} ratio is equal, inside the experimental indetermination, to that obtained in single gas tests, evidence that the observed decrease of the CO_2/CO selectivity in multicomponent conditions is caused by the increase of the CO solubility in the membrane layers when exposed to the CO_2- rich M224 gas mixture.

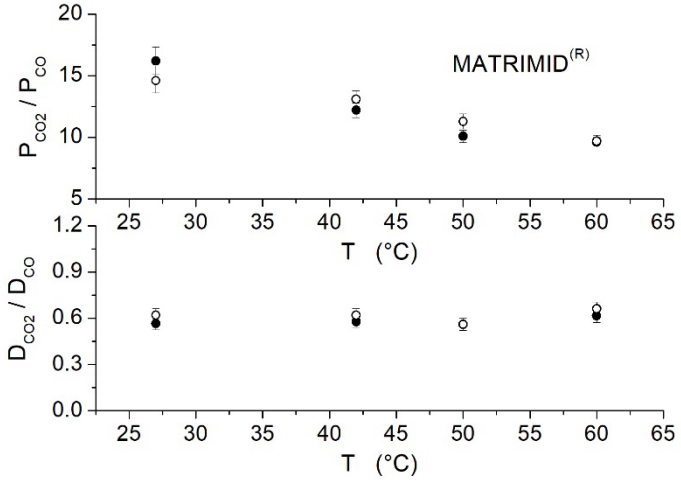

Fig. 9: Matrimid® membrane. Upper panel: CO_2/CO selectivity as a function of temperature. Lower panel: diffusivity ratio D_{CO2}/D_{CO} as a function of temperature. Solid symbols: single gas tests. Open symbols: M224.

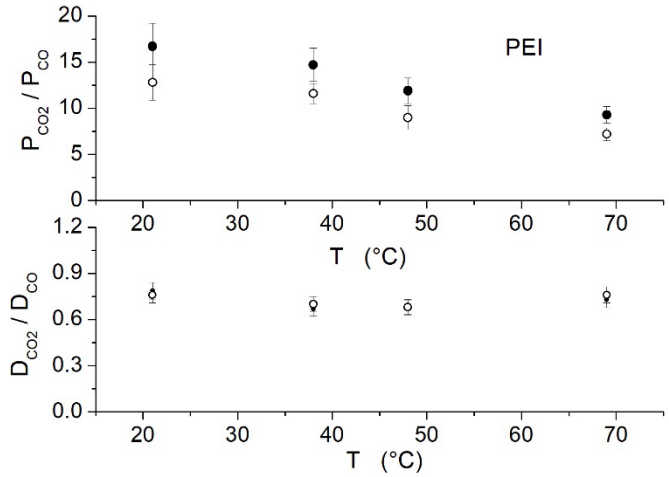

Fig. 10: PEI membrane. Upper panel: CO_2/CO selectivity as a function of temperature. Lower panel: diffusivity ratio D_{CO2}/D_{CO} as a function of temperature. Solid symbols: single gas test. Open symbols: M224.

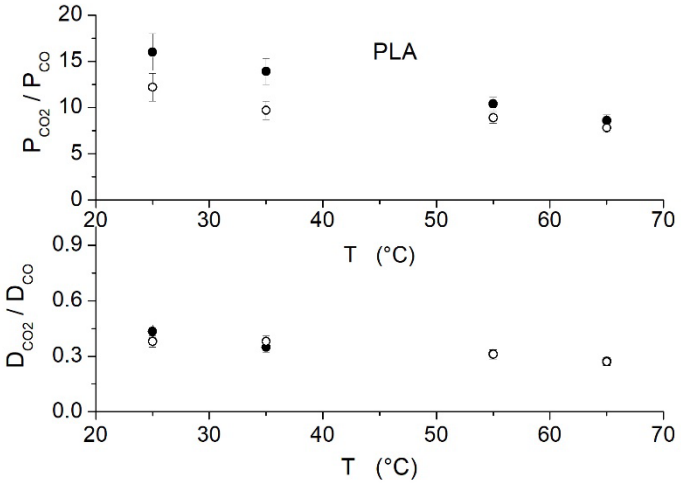

Fig. 11: PLA membrane. Upper panel: CO_2/CO selectivity as a function of temperature. Lower panel: diffusivity ratio D_{CO2}/D_{CO} as a function of temperature. Solid symbols: single gas tests. Open symbols: M224.

Looking at Tab. VIII we observe that the near-ambient temperature P_{CO2} and D_{CO2} values obtained in permeation tests using the quaternary CO_2- lean M225 gas mixture are equal, to within the experimental uncertainty, to the values obtained in single gas tests in all polymers. We also observe that the P_{CO} value results equal, inside its experimental uncertainty, to the value measured in single gas tests and the same occurs with the D_{CO} value. This behavior was observed in the examined temperature range, see tabs. SI1-SI3, indicating that the CO_2/CO selectivity of the examined membrane samples exposed to the quaternary mixture is comparable to the ideal one, maybe due to the lower content of CO_2 in this mixture. The CO_2/CO selectivity decreases, indeed, from 16 ± 1 at near-ambient temperature to 10 ± 1 at 60°C with Matrimid®, from 17 ± 2 at near-

ambient temperature to 10 ± 1 for PEI and from 15 ± 2 at near-ambient temperature to 9 ± 1 at 65°C with PLA.

Comparing CO_2 data obtained in single and mixed gas tests we observe that the presence of CO in the feed gas mixture does not alter the CO_2 transport rates, suggesting that possible interactions of the polar CO molecule with segments of the polymer chains as well as competitive sorption in the polymer layers between CO and CO_2 do not play a role in this transport process. We suggest that the slight increase of the CO solubility with the CO_2- rich M224 feed gas mixture is consequence of the increased overall free volume of the polymer matrix resulting from the dissolved CO_2 molecules. Reasonably the evidence that the CO transport rates are lower with the M225 gas mixture than with the M224 gas mixture approaching those obtained in single gas tests can be attributed to the fact that such mixture contains less CO_2 and the multicomponent effects are less important.

Note that the scientific literature reports only moderate changes between gas permeability values obtained in single gas and in mixed gas tests sometimes observed in studies dedicated to the separation of CO_2/CH_4 binary gas mixtures [37,38]. Furthermore, multicomponent effects are more visible at higher pressures, while the experimental range examined here is sub-atmospheric, as discussed above.

It is worthy to compare the measured CO_2/CO selective performances of the studied membrane samples with literature data. Dense Matrimid® films have been studied by David *et al.*: the authors measured at 303 K in single gas tests with 2 to 6 atm feed pressure a P_{CO2} value of 6.4 Barrer and CO_2/CO ideal selectivity ~ 14 [19]. Scholes et al. studied the separation properties of Matrimid® membranes exposed to gas mixtures (16.2 % CO_2, 9.8 % H_2, 63.2 % N_2, 6.7 % CO, 2.8 % CH_4) and evaluated at 308 K a P_{CO2} value of 7.8 Barrer with CO_2/CO ideal selectivity of 3.3 [39]. Hamidavi et al. studied neat polyetherimide (PEI) films and measured at near-ambient temperature a P_{CO2} value of 0.2 to 0.3 Barrer with ideal selectivity of 6: the authors evaluated a CO activation energy value for permeation of 78.72 kJ/mol in the 300 to 328 K temperature interval [30]. These data are presented in fig. 12 together with selectivity data obtained in the present study: for sake of comparison here we also present CO_2/CO selectivity values vs. P_{CO2} values obtained from a paper by Michaels et al. dedicated to a study of the flow of gases through polyethylene (PE) films with different crystalline content [40]. This figure also shows literature data on the CO_2/CO separation

properties of amorphous polymeric membranes prepared using different kind of fluorinated and non–fluorinated polyimides measured in single gas tests at 323 K with 10 atm feed pressure [41,42] and at 298 K [43], data obtained by Cao et al. in a study on the permeation of gases through polyurethane-polycarbonate membranes at 308 K in single gas tests [44], data pertinent to rubbery poly(dimethylsiloxane) (PDMS), to a glassy PTMSP poly(1-trimethylsilyl-1-propyne) (PTMSP) membrane exposed at 308 K to a simulated syngas (1.5 % H_2S, 10.5 % CO_2, 46% CO and 42 % H_2) [45] and to rubbery polyether-polyamine (Pebax) membranes at 308 K with 10 atm feed pressure in single gas conditions [46]. More detailed information can be found in the Supplementary Information section, see Tab. SI4.

Fig. 12 contains also the upper bond correlation among selectivity and permeability for the separation of the gas couple CO_2/CO, in the trade-off correlation (Robeson's plot), proposed in this work for the first time. It is noteworthy that such upper bound line in the log-log plot was determined in a purely empirical fashion, similarly to the original reference and was found to be $\alpha = 54/P^{0.21}$ [47,48]. It appears from the plot that Matrimid® does not lie exactly on the upper bound but has intermediate values of permeability and selectivity that could make it a good candidate for the removal of CO_2 from CO- containing streams, such as those coming from NTP conversion

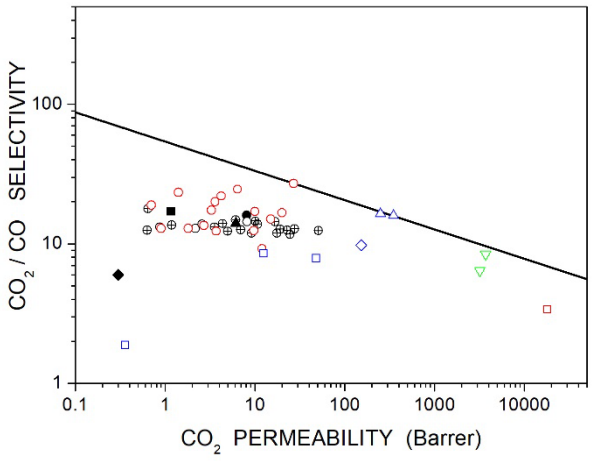

Fig. 12: CO_2/CO selectivity vs. CO_2 permeability. Continuous line refers to the proposed upper-bound correlation similar to the Robeson's plot curve [47,48]. Solid black circle and solid black squares refer to the Matrimid® and PEI films tested in the present study. Open black triangle: Matrimid® film [19]. Open black diamond: Ultem® film [30]. Crossed circles: polyimide films [41,42]. Open red circles: polyurethane-polycarbonate films [44]. Open blue squares: polyethylene films [40]. Open blue diamond: natural rubber [40]. Open blue triangles: polyether-polyamine films [46]. Open red square: poly(1-trimethylsilyl-propyne) film [45]. Open green triangle: polydimethyl siloxane films [45].

Conclusions

The pure and mixed gas permeation of CO_2- rich gas mixtures containing CO, O_2 and N_2 have been investigated for Matrimid®, PEI and PLA membrane films with the aim of exploring such materials in the purification of mixtures coming from the process of CO_2 reforming by non-thermal plasma. Data were obtained with a novel mass spectrometric apparatus which allows to monitor accurately the permeate mixture composition as a function of time, and thus obtained multicomponent diffusivity and permeability values. Single-gas tests indicate that the examined membrane samples present near-ambient temperature values ~ 17 for the ideal CO_2/CO selectivity offering the Matrimid® membrane the highest CO permeability value, 0.50 ± 0.03 Barrer. Increasing temperature, the ideal CO_2/CO selectivity of all samples decreases reaching Matrimid® a selectivity value of ~ 10 at 60°C. In the studied membrane samples the CO_2/CO selectivity has a solution-selective character. Indeed, CO_2 is always the more permeable component in the mixture despite having a smaller diffusivity than CO, thanks to its high solubility in the polymers, which is largely due to its higher condensability. The CO_2/CO selectivity decreases with temperature for all polymers, which is consistent with previous data on other polymers and with the fact that the CO_2 sorption has a larger exothermic effect than that of CO. The CO_2 permeability and diffusivity values do not show significant variations compared to single gas tests using CO_2- rich gases as feed mixture and only a limited increase of the CO transport rate is observed in the presence of high amounts of CO_2 in the mixture.

A tentative Robeson's upper bound has been drawn for the CO_2/CO mixture for which there is lack of data in the literature, and very poor analysis of the obtained results. By looking at this plot, it can be concluded that Matrimid®, lying approximately at the middle of the curve with intermediate values of permeability and selectivity could be a good candidate as membrane for the removal of CO_2 from mixtures containing CO, such as those coming from plasma reformed mixtures and syngas.

References

[1] B. Ashford, Y. Wang, L. Wang and X. Tu, in *Plasma Catalysis, Fundamentals and Applications*, X. Tu, J. C. Whitehead and T. Nozaki (Springer Nature, Switzerland, 2019).

[2] R. Snoeckx and A. Bogaerts, *Plasma technology – a novel solution for CO_2 conversion?* Chem. Soc. Rev. **46** (2017) 5805–5863.

[3] S. D. Kenarsari, D. Yang, G. Jiang, S. Zhang, J. Wang, A. G. Russel, Q. Wei and M. Fan, *Review of recent advances in carbon dioxide separation and capture*, RCS Adv. **3** (2013) 22739-22773.

[4] A. Brunetti, P. Bernardo, G. Barbieri, *Membrane Engineering: Progress and Potentialities in gas Separation*, in: Y. Yampolskii and B. Freeman (Eds.), *Membrane Gas Separation*, John Wiley and Sons, Chichester, 2010, pp.281.
[5] C. Higman and M. van der Burgt, *Gasification* (Elsevier, London, 2008)
[6] M. Monteleone, A. Fuoco, E. Esposito, I. Rose, J. Chen, B. Comesana-Gandara, C. G. Bezzu, M. Carta, N. B. Mckeown, M. G. Shaligyn, V. V. Teplyakov and J. C. Jansen, *Advanced methods for analysis of mixed gas diffusion in polymeric membranes*, J. Membrane Sci. **648** (2022) 120356.
[7] H. Ohya, V. V. Kudruavtsev and S. I. Semenova, *Polyimides Membranes* (Gordon and Breach Publishers: Amsterdam, The Netherlands 1996).
[8] M. J. Troughton*, Handbook of plastic joining: a practical guide*, Elsevier Inc., 2008.
[9] A. Farah, D. G. Anderson and R. Langer, *Physical and mechanical properties of PLA and their functions in widespread applications – a comprehensive review*, Adv. Drug Delivery Rev. **107** (2016) 367-392.
[10] X. Y. Chen, S. Kaliaguine and D. Rodrigue, *A Comparison between Several Commercial Polymer Hollow Fiber Membranes for Gas Separation*, J. Mem. Sep. Technol. **6** (2017) 1-15.
[11] E. Esposito, L. Dellamuzia, U. Moretti, A. Fuoco, L. Giorno and J. C. Jansen, *Simultaneous production of biomethane and food grade CO2 from biogas: an industrial case study*, Energy Environ. Sci. **12** (2019) 281-289.
[12] S. R. Reijerkerk, K. Nijmeijer, C. P. Ribeiro, B. D. Freeman and M. Wessling *On the effects of plasticization in CO_2/light gas separation using polymeric solubility selective membranes* J. Membrane Sci. **2011**, 367, 33–44 ; R. Swaidan, B. Ghanem, M. Al-Saeedi, E. Litwiller, I. Pinnau, *Role of intrachain rigidity in the plasticization of intrinsically microporous triptycene-based polyimide membranes in mixed-gas CO_2/CH_4 separations*, Macromolecules **2014**, 47, 7453–7462 ; G. Genduso, B. S. Ghanem amd I. Pinnau, *Experimental mixed-gas permeability, sorption and diffusion of CO_2-CH_4 mixtures in 6FDA-MPDA polyimide membranes: unveiling the effect of competitive sorption on permeability selectivity*, Membranes 2019 Jan, 9(1). doi: 10.3390/membranes9010010.
[13] L. M. Martini, S. Lovascio, G. Dilecce and P. Tosi, *Time-Resolved CO_2 Dissociation in a Nanosecond Pulsed Discharge*, Plasma Chem. Plasma Proc. **38** (2018) 707-718.
[14] L. M. Martini, N. Gatti, G. Dilecce, M. Scotoni, P. Tosi *Rate constants of quenching and vibrational relaxation in the OH ($A^2\Sigma^+$, $v = 0, 1$) manifold with various colliders,* J. Phys. D Appl. Phys. **50** (2017) 114003.
[15] P. A. Redhead, J. P. Hobson and E. V. Kornelsen, *The Physical Basis of Ultrahigh Vacuum* (AIP, New York, 1993).
[16] R. Checchetto, *Accurate monitoring of gas mixture transport kinetics through polymeric membranes*, Sep. Purif. Technol. **277** (2021) 119477.
[17] J. G. Wijmans and R. W. Backer, *The solution-diffusion model: a review*, J. Membrane Sci. **107** (1995) 1-21.
[18] M. Dickerman, S. Tarter, W. Egger, A. Pegoretti, D. Rigotti, R. S. Brusa and R. Checchetto, *Interface nanocavities in poly(lactic acid) membranes with dispersed cellulose nanofibrils: their role in the gas barrier performances*, Polymer **202** (2020) 122729.
[19] O. C. David, D. Gorri, A. M. Urtiaga and I. Ortiz, *Mixed gas separation study for the hydrogen recovery from H2/CO/N2/CO2 post combustion mixtures using a Matrimid membrane*, J. Membrane Sci. **378** (2011) 359-368.
[20] Y. Zhang, K. J. Balkus Jr., I. H. Musselman and J. P. Ferraris, *Mixed-matrix membranes composed of Matrimid and mesoporous ZSM-5 nanoparticles*, J. Membrane Sci. **325** (2008) 28-39.
[21] S. Shishatskiy, C. Nestor, M. Popa, S. P. Nunes and K. V. Peinemann, *Polyimide asymmetric membranes for hydrogen separation: influence of formation conditions on gas transport properties*, Adv. Eng. Mater. **8** (2006) 390-397.
[22] A. Mirzaei, A. H. Navarchian and S. Tangestaninejad, *Mixed matrix membranes on the basis of Matrimid and palladium zeolitic imidazolate framework for hydrogen separations*, Iran. Polym. J. **29** (2020) 479-491.
[23] A. L. Khan, K. X. Li and Ivo F. J. Vankelecom, *SPEEK/Matrimid blend membranes for CO_2 separation*, J. Membrane Sci. **380** (2011) 55-62.
[24] N. M. Larocca and L. A. Pessan *Effect of antiplasticization on the volumetric, gas sorption and transport properties of polyetherimide*, J. Membrane Sci. **218** (2003) 69-92.

[25] T. A. Barbari, W. J. Koros and D. R. Paul, *Polymeric membranes based on bisphenol-a for gas separation*, J. Membrane Sci. **42** (1989) 69-86.
[26] I. Hao, P. Li and T. S. Chun, *PIM-1 as an organic filler to enhance the gas separation performances of Ultem polyetherimide,* J. Membrane Sci. **453** (2014) 614-623.
[27] Y. Dai, J. R. Johnson, O. Karvan, D. S. Sholl, W. J. Koros, *Ultem®/ZIF-8 mixed hollow fiber matrix membranes for CO2/N2 separations*, J. Membrane Sci. **401-402** (2012) 76-82.
[28] C. Duan, G. Kang, D. Liu, L. Wang, C. Jiangand Q. Yuan, *Enhanced gas separation properties of metal organic framework/polyetherimide mixed matrix membranes*, J. Appl. Polym. Sci. **131** (2014) 8828-8837.
[29] J. Vega, A. Andrio, A. A. Lemus, J. A. I. Diaz, L. F. del Castillo, R. Gavara and V. Compan, *Modification of polyeherimide membranes with ZIFs fillers for CO_2 separation*, Sep. Purif. Technol. **212** (2019) 474-482.
[30] F. Hamidavi, A. Kargari and A. Eliassi, *Sorption and permeation study of polyetherimide/hydrophobic silica nanocomposite membranes for effective syngas (H_2/CO/CO_2 separation*, Sep. Purif. Technol. **279** (2021) 119774.
[31] X. Y. Chen, S. Kaliaguine and D. Rodrigue, *A Comparison between Several Commercial Polymer Hollow Fiber Membranes for Gas Separation*, J. Mem. Sep. Technol. **6** (2017) 1-15.
[32] L. Bao, J. R. Dorgan, D. Knauss, S. hait, N. S. Oliver and I. M. Maruccho, *Gas permeation properties of poly(lactic acid) revisited*, J. Membrane Sci. **285** (2006) 166-172.
[33] T. Komatsuka, A. Kusakabe and K. Nagai, *Characterization and gas transport properties of poly(lactic acid) blend membranes*, Desalination **234** (2008) 212-220.
[34] R. A. Auras, B. Harte, S. Selke and R. Hernandez, *Mechanical, physical, and barrier properties of poly(lactic acid) films*, J. Plas. Films Sheet. **19** (2003) 123-135.
[35] R. Castro-Munoz, V. Martin-Gil, M. Z. Ahmad and V. Fila, *Matrimid 5218 in preparation of membranes for gas separation: current state-of-art*, Chem. Eng. Comm. **205** (2017) 161-196.
[36] H. Y. Zhao, Y. M. Cao, X. L. Ding, M. Q. Zhou, Q. Yuan, *Effects of cross-linkers with different moleculer weights in cross-linked Matrimid 5218 and test temperature on gas transport properties*, J. Membrane Sci. **323** (2008) 176-184.
[37] Y. Zhang, K. J. Balkus Jr., I. H. Musselman and J. P. Ferraris, *Mixed-matrix membranes composed of Matrimid and mesoporous ZSM-5 nanoparticles*, J. Membrane Sci. **325** (2008) 28-39.
[38] S. Shahid and K. Nijmeijer, *Performance and plasticization of polymer-MOF membranes for gas separation at elevated pressures*, J. Membrane Sci. **470** (2014) 166-177.
[39] C. A. Scholes, G. Q. Chen, W. X. Tao, J. Bacus, C. Anderson, G. W. Stevens and S. E. Kentish, *The effect of minor components on the gas separation performances of membranes for carbon capture*, Energy Procedia **4** (2011) 681-687.
[40] A. S. Michaels and H. J. Bixler, *Flow of gases through polyethylene*, J. Polym. Sci. **1** (1961) 413-439.
[41] K. Tanaka, H. Kita, K. Okamoto, A. Nakamura and Y. Kusuki, *Gas permeabiliuty and permselectivity in polyimides based on 3,3', 4,4' –biphenyltetracarboxylic dianhydride* , J. Membrane Sci. **47** (1989) 203-215
[42] [K. Tanaka, H. Kita, M. Okano and K.Okamoto, *Permeability and permeselctivity of gases in fluorinated and non-fluorinated polyimides*, Polymer **33** (1992) 585-592
[43] K. Haraya, K. Obata, T. Hakuta and H. Yoshitome, *The permeation of gases through a new type of polyimide membranes*, Membrane **11** (1986) 48-52
[44] N. Cao, M. Pegoraro, F. Bianchi, L. Di Landro and L. Zanderighi, *Gas transport properties of polycarbonate-polyuretane membranes*, J. Appl. Polym. Sci. **48** (1993) 1831-1842
[45] T. C. Merkel, R. P. Gupta, B. S. Turk and B. D. Freeman, *Mixed gas permeation if syngas components in poly(dimethylsiloxane) and poly(1-trimetyhylsilyl-1-popyne) at elevated temperature,* J. Membrane Sci. **191** (2001) 85-94.
[46] B. Wilks and M. E. Rezac, *Properties of rubbery polymers for the recovery of hydrogen sulfide from gasification gases*, J. Appl. Polym. Sci. **85** (2002) 2436-2444.
[47] L. M. Robeson, *Correlation of separation factors versus permeability for polymeric membranes*, J. Membrane Sci. **62** (1991) 165-185.
[48] L. M. Robeson, *The upper bound revisited*, J. Membrane Sci. **320** (2008) 390-400.

SUPPLEMENTARY INFORMATION

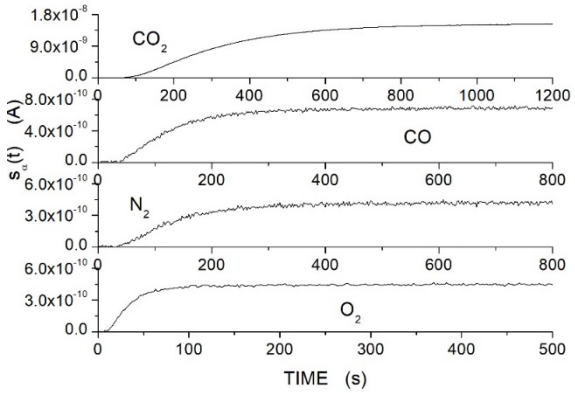

Fig. SI1: $s_\alpha(t)$ mass signals obtained at $T = 300 \pm 2$ K with the PLA film sample exposed to pure CO_2, CO and N_2 gases ($p_{feed} = 45 \pm 1$ kPa) and to the dry N_2/O_2 air mixture ($p_{feed} = 72 \pm 1$ kPa).

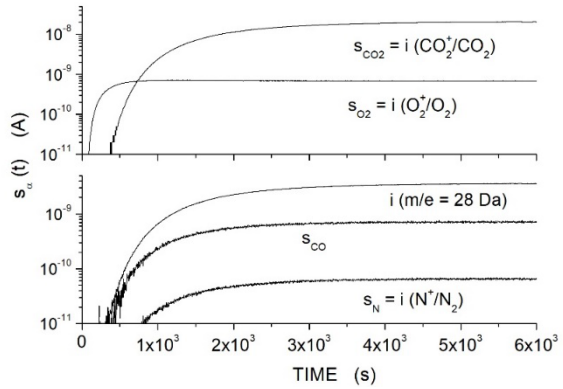

Fig. SI2: $s_\alpha(t)$ mass signals obtained at $T = 300 \pm 2$ K with the PEI film sample exposed to the M224 gas mixture ($p_{feed} = 45 \pm 1$ kPa).

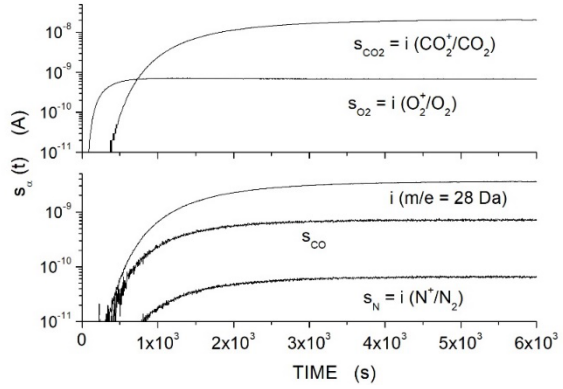

Fig. SI3: $s_\alpha(t)$ mass signals obtained at $T = 300 \pm 2$ K with the Matrimid® film sample exposed to the M225 gas mixture ($p_{feed} = 72 \pm 1$ kPa).

Matrimid®		300 ± 2 K	315 ± 2 K	323 ± 2 K	333 ± 2 K
P_{CO2} (Barrer)	SG	8.1 ± 0.3	9.5 ± 0.3	10.1 ± 0.3	11.1 ± 0.3
	M224	7.9 ± 0.3	9.7 ± 0.3	10.0 ± 0.3	11.3 ± 0.3
	M225	8.0 ± 0.3	9.6 ± 0.3	10.0 ± 0.3	11.2 ± 0.3
P_{CO} (Barrer)	SG	0.50 ± 0.03	0.77 ± 0.03	1.00 ± 0.04	1.14 ± 0.04
	M224	0.54 ± 0.03	0.74 ± 0.03	0.81 ± 0.05	1.16 ± 0.04
	M225	0.49 ± 0.03	0.75 ± 0.03	0.95 ± 0.06	1.13 ± 0.06
D_{CO2} (cm^2/s)	SG	$(2.2 \pm 0.1) \times 10^{-9}$	$(4.1 \pm 0.1) \times 10^{-9}$	$(5.2 \pm 0.2) \times 10^{-9}$	$(8.0 \pm 0.3) \times 10^{-9}$
	M224	$(2.3 \pm 0.1) \times 10^{-9}$	$(4.2 \pm 0.1) \times 10^{-9}$	$(5.0 \pm 0.2) \times 10^{-9}$	$(7.5 \pm 0.3) \times 10^{-9}$
	M225	$(2.1 \pm 0.1) \times 10^{-9}$	$(4.1 \pm 0.1) \times 10^{-9}$	$(5.1 \pm 0.2) \times 10^{-9}$	$(7.6 \pm 0.3) \times 10^{-9}$
D_{CO} (cm^2/s)	SG	$(3.9 \pm 0.2) \times 10^{-9}$	$(7.1 \pm 0.3) \times 10^{-9}$	$(9.3 \pm 0.3) \times 10^{-9}$	$(1.22 \pm 0.05) \times 10^{-8}$
	M224	$(3.7 \pm 0.2) \times 10^{-9}$	$(6.7 \pm 0.3) \times 10^{-9}$	$(9.0 \pm 0.3) \times 10^{-9}$	$(1.14 \pm 0.05) \times 10^{-8}$
	M225	$(3.8 \pm 0.2) \times 10^{-9}$	$(6.8 \pm 0.3) \times 10^{-9}$	$(9.0 \pm 0.3) \times 10^{-9}$	$(1.16 \pm 0.05) \times 10^{-8}$
P_{O2} (Barrer)	SG	1.8 ± 0.1	2.6 ± 0.1	3.1 ± 0.1	3.4 ± 0.1
	M224	1.8 ± 0.1	2.6 ± 0.1	3.0 ± 0.1	3.4 ± 0.2
	M225	1.7 ± 0.1	2.7 ± 0.1	3.0 ± 0.1	3.3 ± 0.1
D_{O2} (cm^2/s)	SG	$(1.7 \pm 0.1) \times 10^{-8}$	$(2.7 \pm 0.1) \times 10^{-8}$	$(3.2 \pm 0.1) \times 10^{-8}$	$(4.5 \pm 0.1) \times 10^{-8}$
	M224	$(1.7 \pm 0.1) \times 10^{-8}$	$(2.7 \pm 0.1) \times 10^{-8}$	$(3.1 \pm 0.1) \times 10^{-8}$	$(3.9 \pm 0.2) \times 10^{-8}$
	M225	$(1.7 \pm 0.1) \times 10^{-8}$	$(2.8 \pm 0.1) \times 10^{-8}$	$(3.2 \pm 0.1) \times 10^{-8}$	$(4.2 \pm 0.2) \times 10^{-8}$
P_{N2} (Barrer)	SG	0.29 ± 0.02	0.44 ± 0.02	0.50 ± 0.02	0.65 ± 0.02
	M225	0.27 ± 0.03	0.42 ± 0.03	0.51 ± 0.03	0.64 ± 0.03
D_{N2} (cm^2/s)	SG	$(3.4 \pm 0.2) \times 10^{-9}$	$(5.9 \pm 0.2) \times 10^{-9}$	$(8.0 \pm 0.2) \times 10^{-9}$	$(1.10 \pm 0.03) \times 10^{-9}$
	M225	$(3.4 \pm 0.3) \times 10^{-9}$	$(6.0 \pm 0.3) \times 10^{-9}$	$(8.3 \pm 0.3) \times 10^{-9}$	$(1.10 \pm 0.05) \times 10^{-9}$

Tab. SI1: Permeability and diffusivity numerical values of CO_2, O_2, N_2 and CO in the Matrimid® membrane sample (p_{feed} = 20 to 90 kPa).

PEI		295 ± 2 K	311 ± 2 K	321 ± 2 K	342 ± 2 K
P_{CO2} (Barrer)	SG	1.17 ± 0.05	1.18 ± 0.05	1.19 ± 0.05	1.24 ± 0.05
	M224	1.15 ± 0.05	1.16 ± 0.05	1.17 ± 0.05	1.22 ± 0.05
	M225	1.17 ± 0.05	1.16 ± 0.05	1.18 ± 0.05	1.24 ± 0.05
P_{CO} (Barrer)	SG	0.07 ± 0.01	0.08 ± 0.01	0.10 ± 0.01	0.12 ± 0.01
	M224	0.09 ± 0.01	0.10 ± 0.01	0.13 ± 0.01	0.17 ± 0.01
	M225	0.07 ± 0.01	0.09 ± 0.01	0.11 ± 0.01	0.12 ± 0.01
D_{CO2} (cm^2/s)	SG	$(8.5 \pm 0.4) \times 10^{-9}$	$(1.20 \pm 0.05) \times 10^{-8}$	$(1.7 \pm 0.1) \times 10^{-8}$	$(2.7 \pm 0.1) \times 10^{-8}$
	M224	$(8.0 \pm 0.4) \times 10^{-9}$	$(1.20 \pm 0.05) \times 10^{-8}$	$(1.5 \pm 0.1) \times 10^{-8}$	$(2.8 \pm 0.1) \times 10^{-8}$
	M225	$(8.1 \pm 0.4) \times 10^{-9}$	$(1.20 \pm 0.05) \times 10^{-8}$	$(1.7 \pm 0.1) \times 10^{-8}$	$(2.8 \pm 0.1) \times 10^{-8}$
D_{CO} (cm^2/s)	SG	$(1.08 \pm 0.04) \times 10^{-8}$	$(1.95 \pm 0.07) \times 10^{-8}$	$(2.5 \pm 0.1) \times 10^{-8}$	$(3.7 \pm 0.1) \times 10^{-8}$
	M224	$(1.05 \pm 0.04) \times 10^{-8}$	$(1.72 \pm 0.07) \times 10^{-8}$	$(2.2 \pm 0.1) \times 10^{-8}$	$(3.7 \pm 0.1) \times 10^{-8}$
	M225	$(1.03 \pm 0.04) \times 10^{-8}$	$(1.81 \pm 0.07) \times 10^{-8}$	$(2.4 \pm 0.1) \times 10^{-8}$	$(3.6 \pm 0.1) \times 10^{-8}$
P_{O2} (Barrer)	SG	0.32 ± 0.02	0.35 ± 0.02	0.38 ± 0.02	0.50 ± 0.02
	M224	0.30 ± 0.02	0.34 ± 0.02	0.37 ± 0.02	0.49 ± 0.02
	M225	0.32 ± 0.02	0.35 ± 0.02	0.37 ± 0.02	0.50 ± 0.02
D_{O2} (cm^2/s)	SG	$(3.6 \pm 0.1) \times 10^{-8}$	$(5.0 \pm 0.1) \times 10^{-8}$	$(6.0 \pm 0.1) \times 10^{-8}$	$(9.5 \pm 0.1) \times 10^{-8}$
	M224	$(3.5 \pm 0.1) \times 10^{-8}$	$(5.1 \pm 0.1) \times 10^{-8}$	$(6.0 \pm 0.1) \times 10^{-8}$	$(9.3 \pm 0.1) \times 10^{-8}$
	M225	$(3.4 \pm 0.1) \times 10^{-8}$	$(5.2 \pm 0.1) \times 10^{-8}$	$(6.1 \pm 0.1) \times 10^{-8}$	$(9.5 \pm 0.1) \times 10^{-8}$
P_{N2} (Barrer)	SG	0.04 ± 0.01	0.04 ± 0.01	0.05 ± 0.01	0.07 ± 0.01
	M225	0.05 ± 0.02	0.04 ± 0.02	0.05 ± 0.01	0.07 ± 0.01
D_{N2} (cm^2/s)	SG	$(1.01 \pm 0.03) \times 10^{-8}$	$(2.00 \pm 0.03) \times 10^{-8}$	$(2.24 \pm 0.03) \times 10^{-8}$	$(3.51 \pm 0.03) \times 10^{-8}$
	M225	$(1.1 \pm 0.1) \times 10^{-8}$	$(2.0 \pm 0.1) \times 10^{-8}$	$(2.3 \pm 0.1) \times 10^{-8}$	$(3.4 \pm 0.1) \times 10^{-8}$

Tab. SI. 2: Permeability and diffusivity numerical values of CO_2, O_2, N_2 and CO in the PEI membrane sample (p_{feed} = 20 to 90 kPa).

PLA		298 ± 2 K	308 ± 2 K	328 ± 2 K	338 ± 2 K
P_{CO2} (Barrer)	SG	1.12 ± 0.05	1.39 ± 0.05	2.5 ± 0.1	3.2 ± 0.1
	M224	1.10 ± 0.05	1.35 ± 0.05	2.5 ± 0.1	3.1 ± 0.1
	M225	1.10 ± 0.05	1.37 ± 0.05	2.6 ± 0.1	3.1 ± 0.1
P_{CO} (Barrer)	SG	0.07 ± 0.01	0.10 ± 0.01	0.24 ± 0.01	0.37 ± 0.02
	M224	0.09 ± 0.01	0.14 ± 0.01	0.28 ± 0.01	0.40 ± 0.02
	M225	0.08 ± 0.02	0.12 ± 0.02	0.25 ± 0.02	0.38 ± 0.02
D_{CO2} (cm^2/s)	SG	$(4.0 \pm 0.2) \times 10^{-9}$	$(5.6 \pm 0.2) \times 10^{-9}$	$(1.68 \pm 0.06) \times 10^{-8}$	$(2.4 \pm 0.1) \times 10^{-8}$
	M224	$(3.8 \pm 0.2) \times 10^{-9}$	$(5.7 \pm 0.2) \times 10^{-9}$	$(1.60 \pm 0.06) \times 10^{-8}$	$(2.4 \pm 0.1) \times 10^{-8}$
	M225	$(3.8 \pm 0.2) \times 10^{-9}$	$(5.7 \pm 0.2) \times 10^{-9}$	$(1.62 \pm 0.06) \times 10^{-8}$	$(2.4 \pm 0.1) \times 10^{-8}$
D_{CO} (cm^2/s)	SG	$(9.2 \pm 0.4) \times 10^{-9}$	$(1.61 \pm 0.08) \times 10^{-8}$	$(5.4 \pm 0.2) \times 10^{-8}$	$(8.7 \pm 0.3) \times 10^{-8}$
	M224	$(1.00 \pm 0.04) \times 10^{-8}$	$(1.50 \pm 0.06) \times 10^{-8}$	$(5.2 \pm 0.2) \times 10^{-8}$	$(9.0 \pm 0.4) \times 10^{-8}$
	M225	$(9.7 \pm 0.6) \times 10^{-9}$	$(1.55 \pm 0.06) \times 10^{-8}$	$(5.1 \pm 0.2) \times 10^{-8}$	$(8.7 \pm 0.4) \times 10^{-8}$
P_{O2} (Barrer)	SG	0.29 ± 0.02	0.40 ± 0.02	0.73 ± 0.04	1.04 ± 0.04
	M224	0.30 ± 0.02	0.41 ± 0.02	0.70 ± 0.04	0.92 ± 0.05
	M225	0.30 ± 0.02	0.40 ± 0.03	0.71 ± 0.04	0.95 ± 0.05
D_{O2} (cm^2/s)	SG	$(4.3 \pm 0.2) \times 10^{-8}$	$(6.0 \pm 0.2) \times 10^{-8}$	$(1.8 \pm 0.1) \times 10^{-7}$	$(2.5 \pm 0.1) \times 10^{-7}$
	M224	$(4.1 \pm 0.2) \times 10^{-8}$	$(7.1 \pm 0.2) \times 10^{-8}$	$(1.8 \pm 0.1) \times 10^{-7}$	$(2.4 \pm 0.1) \times 10^{-7}$
	M225	$(4.1 \pm 0.2) \times 10^{-8}$	$(7.0 \pm 0.2) \times 10^{-8}$	$(1.9 \pm 0.1) \times 10^{-7}$	$(2.3 \pm 0.1) \times 10^{-7}$
P_{N2} (Barrer)	SG	0.05 ± 0.01	0.07 ± 0.01	0.19 ± 0.01	0.26 ± 0.02
	M225	0.04 ± 0.01	0.06 ± 0.01	0.20 ± 0.02	0.26 ± 0.03
D_{N2} (cm^2/s)	SG	$(7.1 \pm 0.4) \times 10^{-9}$	$(1.2 \pm 0.1) \times 10^{-8}$	$(4.0 \pm 0.2) \times 10^{-8}$	$(6.1 \pm 0.3) \times 10^{-8}$
	M225	$(7.0 \pm 0.3) \times 10^{-9}$	$(1.1 \pm 0.2) \times 10^{-8}$	$(4.0 \pm 0.3) \times 10^{-8}$	$(6.0 \pm 0.4) \times 10^{-8}$

Tab. SI. 3: Permeability and diffusivity numerical values of CO_2, O_2, N_2 and CO in the PLA membrane sample (p_{feed} = 20 to 90 kPa).

Membrane sample	P_{CO2} (barrer)	P_{CO2}/P_{CO} (*)	E_P^{CO2} (kJ/mol)	E_P^{CO} (kJ/mol)	Test conditions	Ref.
Matrimid®	8.1 ± 0.3	17 ± 1	7.7 ± 0.5	20.7 ± 0.9	SG	This work
PEI	1.17 ± 0.05	17 ± 1	1.0 ± 0.2	9.3 ± 0.5	SG	This work
PLA	1.12 ± 0.05	16 ± 1	22.4 ± 0.5	36 ± 1	SG	This work
Matrimid®	6.1	14	8.1	16.5	SG	[39]
Ultem® 1000	0.3	6	34.37	78.72	SG	[30]
PE (Grex)	0.36	1.87	30.15	39.37	SG	[40]
PE (Alathon)	12.63	8.50	38.95	46.49	SG	[40]
PE (Hydropol)	48.42	7.83	36.44	44.81	SG	[40]
Natural rubber	154	9.75	21.78	31	SG	[40]
PDMS	3200	6.4	2.2	11	GM (**)	[36]
PTMSP	18200	3.4	-6.5	-2.1	GM (**)	[36]
Pebax 2533	350	15.9	6.5	19.4	SG	[46]
Polyimide	1.48	22.7	12.8	23.4	SG	[43]

Tab. SI4

(*) P_{CO2}/P_{CO} values measured at near-ambient temperature.

SG: Single Gas

(**) GM: Gas mixture 1.5 % H_2S, 10.5 % CO_2, 46% CO and 42 % H_2